Journal of Statistical Physics, Vol. 64, Nos. 3/4, 1991

Multifractality of Space-Filling Bearings and Apollonian Packings

S. S. Manna[1] **and T. Vicsek**[1,2]

Received November 30, 1990; final March 25, 1991

We study the structure of space-filling bearings (SFB) and Apollonian packings (AP) by determining the scaling behavior of the density distribution of points where the circles touch each other. Application of the sand box method to the average of the qth power of the number of touching points reveals the multifractal aspects of the structure of SFB and AP.

KEY WORDS: Fractals; multifractals; Apollonian packing; space-filling bearings.

1. INTRODUCTION

During the last decade it has been demonstrated by several theoretical and numerical approaches that the main features of far-from-equilibrium phenomena can be sucessfully captured through their geometrical aspects. The lack of equilibrium and the nonlinearity of such phenomena typically result in intricate shapes, and the description of their development should be based on the detailed understanding of the underlying geometry.[1] Examples falling into this category include a wide selection of fractal growth phenomena[2] (aggregation, dendritic growth, dielectric breakdown), attractors in dynamical systems (e.g., ref. 3), and a rich variety of patterns observed in fluid flows.[4]

A large class of patterns occurring in systems far from equilibrium can be described in terms of units which fill the space, but have a power-law size distribution. Perhaps the earliest example of this kind of geometry was discovered by the ancient Greeks, who called the corresponding structure Apollonian packing (AP). In this construction nonoverlapping circles of

[1] HLRZ, KFA Jülich, 5170 Jülich, Germany.
[2] Permanent address: Department of Atomic Physics, Eötvös University, Budapest, 1445 Hungary.

0022-4715/91/0800-0525$06.50/0

very different radii are used to tile the region bounded by three touching circles. Very recently a related model has been proposed to describe systems which are made of rotating parts filling the space.[5] In this model of space-filling bearings (SFB), cylinders having parallel axes are arranged in space in such a manner that in the limiting case the cylinders completely fill the space and, in addition, they can roll on each other without slipping.

The geometry of plane- or space-filling objects (disks, spheres, and bearings) has a number of potential applications. For example, oil drops on the surface of an immiscible liquid have a number of common features with SFB. Another important field to which space-filling models are closely related is the hydrodynamics of porous media.[6] Furthermore, the model (SFB) in which the condition of frictionless rotation of the cylinders is satisfied is expected[5] to be useful in modeling the structure of turbulent flows in the inertial regime[4] or the motion of the matter in seismic gaps.[7]

In this paper we carry out a multifractal analysis of the structure of space-filling bearings using a formalism which is analogous to the treatment of fractal measures.[8–10] The idea of determining the multifractal spectrum for the case of space-filling structures made of cylinders is motivated by the multiplicative nature of the process which is used to generate these structures. In the next section we describe the methods we applied to obtain the SFB and the Apollonian packing, as well as the procedure used to evaluate the multifractal spectrum. In Section 3 we present our results concerning the multifractal behavior of space-filling bearings and Apollonian packings. The results are discussed in Section 4.

2. METHODS

2.1. Algorithm for Constructing Space-Filling Bearings

In this section we discuss the construction of SFB packing, the algorithm proposed in ref. 5 (see also ref. 18). In the model of space-filling bearings whole space is filled with parallel cylinders which roll on one another without slipping. In a section perpendicular to the length of these cylinders one gets a distribution of circles of many different sizes tangentially touching one another and covering the whole plane. One can imagine a loop or closed path through the touching points of a set of circles touching one another. The condition of slipless rotation demands that two circles which are touching each other must rotate in opposite directions. As a consequence, there can be only an even number of circles in a loop.[5] Loops having four circles give the simplest example of SFB.

SFB packing in a strip geometry is done by an iteration procedure. Given one set of circles, one generates the next smaller set of circles using

circular inversions. In an inversion around a circle of radius r a point is mapped into its image point such that both points lie on the same line connecting the center to infinity and their distances d and d' from the center fulfill $d \cdot d' = r^2$. In complex number notation this transformation is $z \to z' = r^2/z^*$.

We describe here the construction of SFB packing in a strip geometry. The whole packing is periodic and a specific unit repeats at regular interval. One starts with two horizontal infinite lines at unit distance apart and places two seed circles A and B touching each other and the top and bottom lines, respectively. These two lines can be thought of as two circles of infinite radii touching at infinity and together with the seed circles A and B they form the initial fourfold loop of four circles. The whole SFB packing is produced by the two trees of circles generated from these two seed circles. All four loop packings on a strip are divided into two families.[5] In the first family the sum of the radii of A and B is greater than the strip width and in the second family it is equal to the strip width. In the first family there are an infinite number of ways one can fill a strip. Each member of this family is characterized by two nonnegative integer parameters n and m. Given the values of n and m, one finds a set of constants: namely, R_A and R_B, the radii of the seed circles A and B; r_A and r_B, the radii of the inversion circles corresponding to A and B; and the period $2a$.[5] The values of these constants depend on n and m through the following algebraic equations[5]:

$$z_n = \cos^{-2}[\pi/(n+3)] \tag{1}$$

$$a^{-2} = z_n + z_m - 1 \tag{2}$$

$$r_{A,B}^2 = z_{n,m}/(z_n + z_m - 1) \tag{3}$$

$$2R_A = r_A^2, \qquad 2R_B = r_B^2 \tag{4}$$

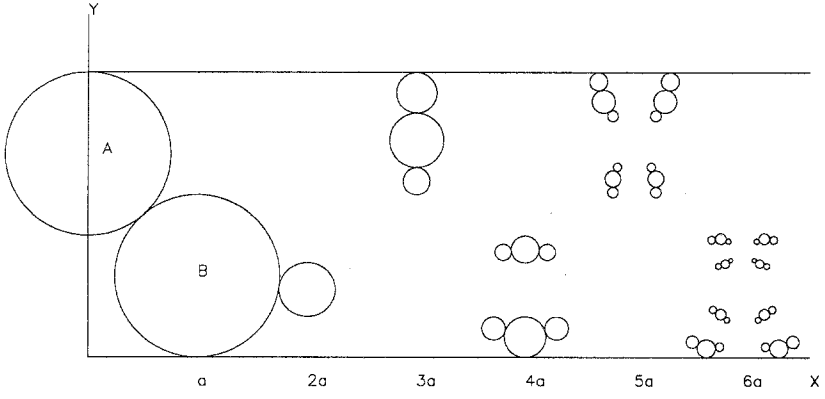

Fig. 1. Construction of space-filling bearings.

We describe here the algorithm for the generation of the member $n = m = 0$, for which $a = 1/\sqrt{7}$, $R_A = R_B = R = 2/7$, and $r_A = r_B = 2/\sqrt{7}$.

The trees of circles following from the seed circles A and B are independent of each other. Therefore we construct the A tree and B tree separately and superpose them (see Fig. 1). The seed circle A is placed on the strip touching the top line. We fix our x axis on the bottom line and y axis passing through the center of the A circle. In the first generation, circle A is inverted around an inversion circle of radius r_A centered at the point $(3a, 0)$ to get the second circle. In the second generation both these circles are inverted at the point $(4a, 1)$ to generate two more circles. In the third generation all these four circles are inverted at the point $(5a, 0)$ to generate another four circles and the process is continued to generate the

(a)

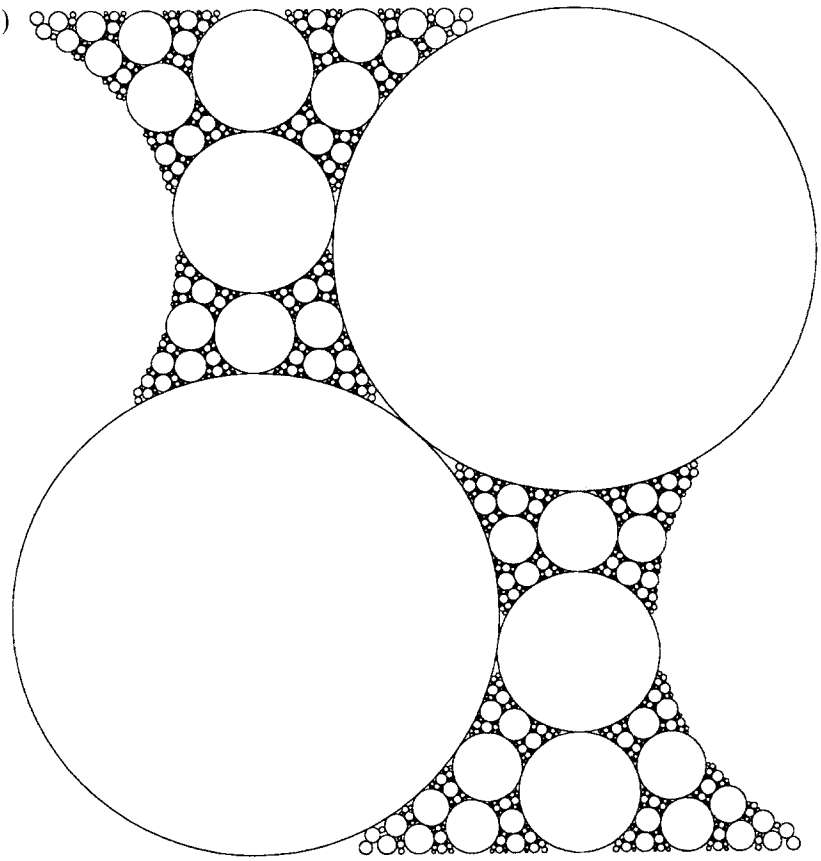

Fig. 2. (a) A typical picture obtained in the course of generating space-filling bearings including the first five steps of the construction (2048 circles). (b) The corresponding set of 4096 touching points.

(b)

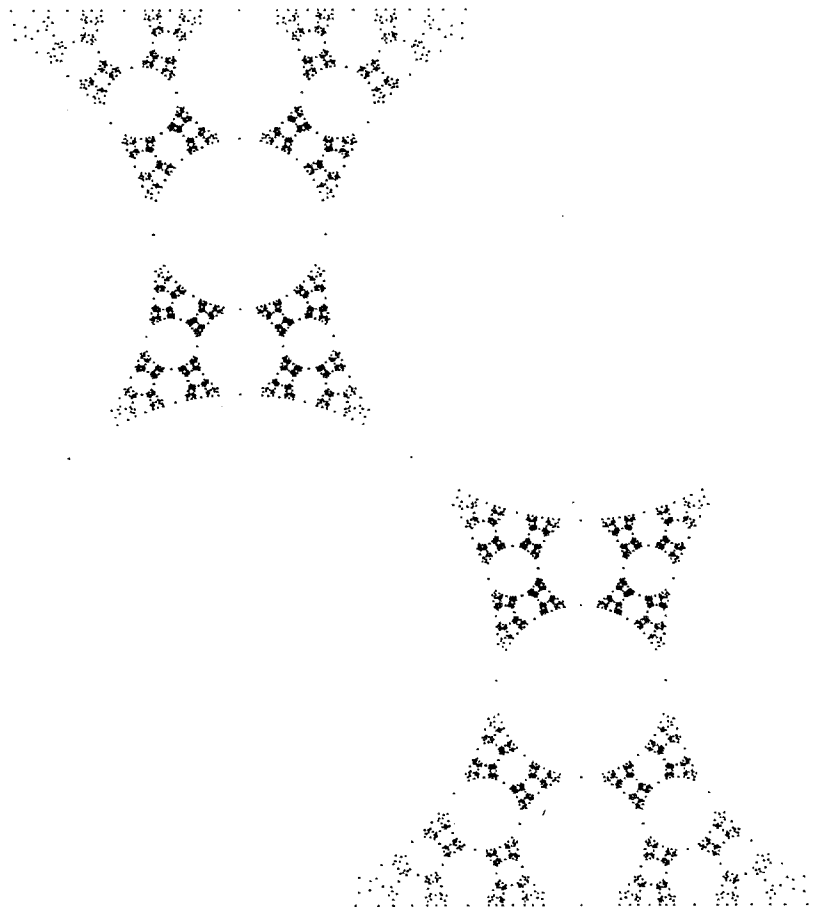

Fig. 2. (*Continued*)

A tree. Next one places the seed circle B with the center at (a, R) and then constructs successive images by inverting at the points $(4a, 1)$, $(5a, 0)$, $(6a, 1)$, and so on and thus the B tree is produced. Finally, all circles are shifted; depending on the generation they are produced by proper translations to be within $x = 0$ and $x = 3a$ (see Fig. 2a).

To generate the touching points, we use the fact that the touching points are mapped into touching points. Therefore, we start, for seed circle A, with two touching points at $(0, 1)$ and $(a/2, 1/2)$ and these points are successively inverted at alternate points at the bottom and top to produce the tree of touching points. Similarly one gets touching points generated from the seed circle B which are at $(a, 0)$ and $(3a/2, 1/2)$. Finally, all points in one generation are shifted to get them in the region within $x = 0$ and $x = 3a$. The resulting picture is shown in Fig. 2b for 4096 points.

The number of circles generated at the kth generation from one seed circle is 2^k. These circles have a distribution of radii. The minimum radius at the kth generation scales as $\lambda_{\min}^{-k}$ and the maximum radius scales as $\lambda_{\max}^{-k}$, where $\lambda_{\min} = 1.883$ and for $\lambda_{\max}$ convergence is poor and seems to approach 1.

2.2. Algorithm for Generating Apollonian Packings

For any set of three circles of radii r_1, r_2, and r_3 which touch one another one gets the radius of a fourth circle which touches the three circles and enclosed by them, using the formula[11]

$$\frac{1}{r} = \frac{1}{r_1} + \frac{1}{r_2} + \frac{1}{r_3} + 2\left(\frac{1}{r_1 r_2} + \frac{1}{r_2 r_3} + \frac{1}{r_3 r_1}\right)^{1/2} \tag{5}$$

The coordinates of the center are then found using coordinate geometry.

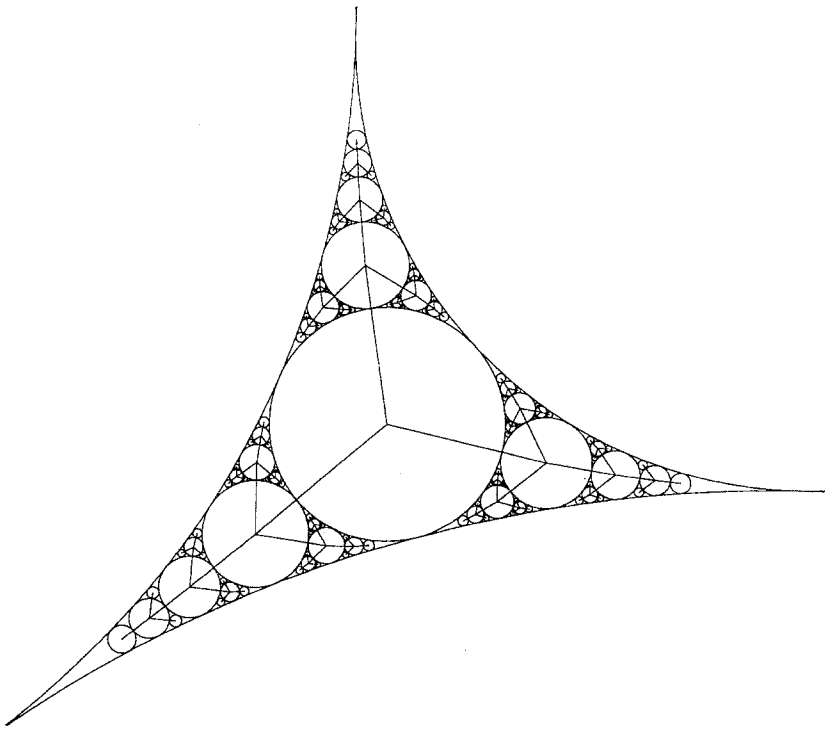

Fig. 3. A typical picture obtained in the course of generating an Apollonian packing. The first six steps of the construction is shown (1096 circles).

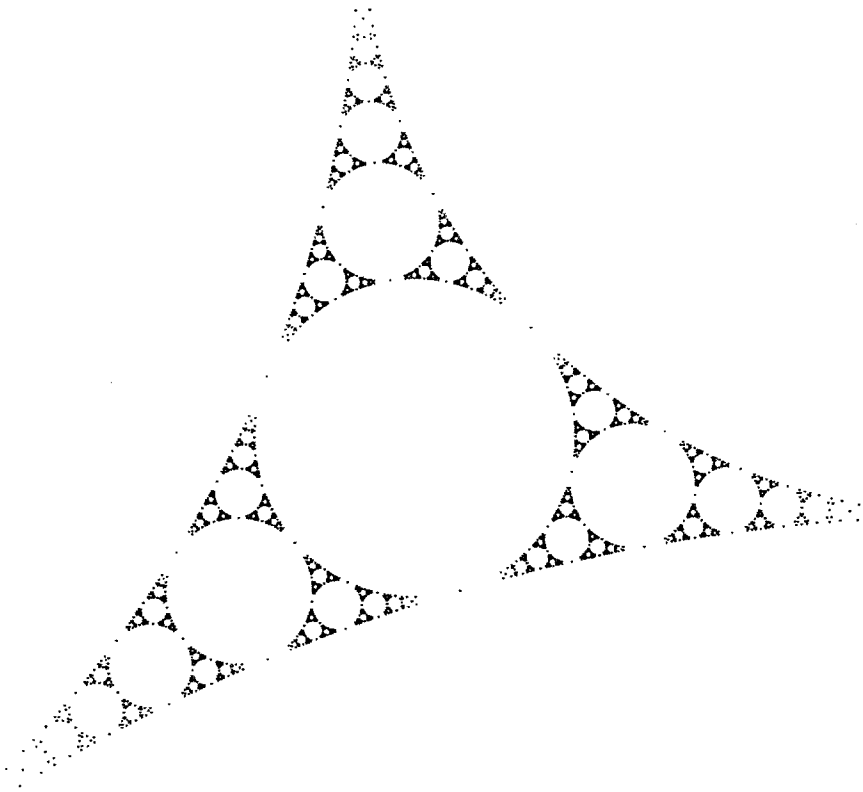

Fig. 4. The set of 3279 touching points corresponding to Fig. 3.

Here we start with three circles of radii 1, 2, and 3 which touch one another. A curved triangle is formed and we place a fourth circle on it. With the fourth circle we have three curved triangles and we start generating other circles in these three regions in the form of a Cayley tree of coordination number three (see Fig. 3). In the first generation we have one circle, the fourth circle mentioned above. In the second generation we have three more circles in the three curved triangles and so on. We use Martin's backtracking algorithm[12] to exactly enumerate all circles produced up to some level of generation. Proper care has been taken to decide the left, front, and right directions in local environments. The set of touching points in Apollonian packing is shown in Fig. 4.

The number of circles generated at the kth generation from the seed circle is 3^k. These circles have a distribution of radii. The minimum radius at the kth generation scales as $\lambda_{\min}^{-k}$, where $\lambda_{\min}$ is $g+\sqrt{g}$, where g is the golden mean.[13] In the Cayley tree structure the branch which always turns

left (right) produces the minimum-radii circles. These radii are obtained by using the radii of the last three parent circles and Eq. (5). The maximum radius decreases with the generation number k as k^{-2}.[11]

2.3. Calculation of the Multifractal Spectrum

In a standard multifractal analysis[14] a grid of lattice constant l is put over the fractal on which the fractal measure is defined and the amount of measure p in the boxes of the grid is determined. Then, from the expression

$$\sum_i p_i^q \sim l^{(q-1)D_q} \tag{6}$$

the infinite hierarchy of exponents can be calculated.

To characterize the multifractal aspects of the structure of a fractal we need to define an appropriate measure. In the case of a geometrical object a natural choice is the Lebesgue measure of the part of the structure in the given region.[15] For the fractals studied in this paper this paper this choice would correspond to the total length of the circles which are within a box of linear size l. Of course, this could be carried out only for a construction with a finite number of iteration steps k, since in the $k \to \infty$ limit the length in each finite part of the fractal becomes infinitely large.

For practical reasons, however, we choose another quantity, which is the number of touching points within a box. It is considerably easier to calculate this quantity, and it provides a basis for an appropriate measure since in the $k \to \infty$ limit the set of touching points and the fractal itself coincide. Thus, we define our measure as $p_i = m_i(l)/m_0$, where $m_i(l)$ is the number of touching points in the ith box of size l and m_0 is the total number of touching points in the structure.

Therefore, our method will describe the multifractal nature of the density distribution of the touching points in space-filling bearings and Apollonian gaskets. The most efficient way to calculate the related generalized dimensions D_q is based on the sand-box method in which the average of the qth moments of the distribution of p_i values is determined for boxes of varying sizes centered at randomly selected points belonging to the structure.[16] We shall use circles of radii r instead of boxes. Choosing the centers randomly and taking an average over the observed m_i does not correspond exactly to Eq. (6), since in this way the places with a higher density of touching points are represented with a larger weight. Correspondingly, instead of (6) the following expression has to be used:

$$\chi_q(r) = \left\langle \left(\frac{m_i(r)}{m_0} \right)^{q-1} \right\rangle \sim r^{(q-1)D_q} \tag{7}$$

When using the above equation, the condition $r_{\min} \ll r \ll 1$ has to be satisfied in order to obtain reliable data. This method has been successful in demonstrating the multifractal geometry of asymmetric Cantor sets[16] and diffusion-limited aggregates.[17]

If the D_q values are known, the multifractal spectrum $f(\alpha)$ as a function of the local mass exponent $\ln(m_i/m_0)/\ln r$ can be calculated using the equations[9,10]

$$(q-1)\,D_q = q\alpha(q) - f(\alpha(q)), \qquad \alpha(q) = (d/dq)[(q-1)\,D_q]$$

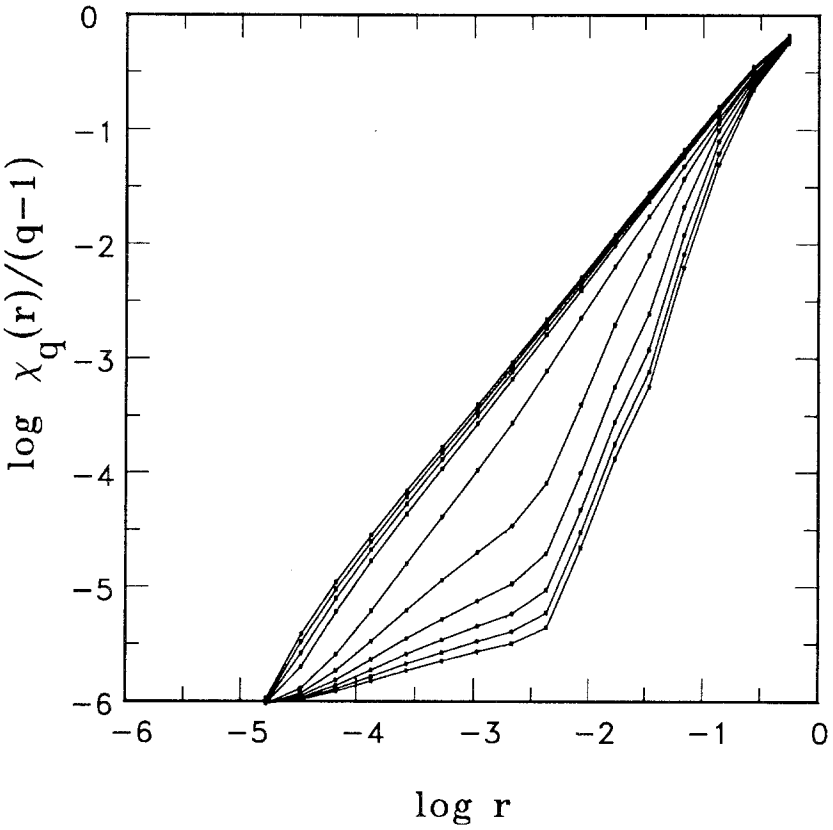

Fig. 5. The multifractal scaling of the distribution of the touching points demonstrated for the construction shown in Fig. 2b. The generalized dimensions D_q can be determined from the slopes of the straight lines fitted to the data on the interval $-2.3 < \log r < -0.6$ for $q < 0$ and on the interval $-4 < \log r < -0.6$ for $q \geqslant 0$.

3. RESULTS

3.1. D_q Spectrum for Space-Filling Bearings

The generalized dimensions D_q associated with the multifractal scaling of the distribution of touching points in space-filling bearings were calculated for a structure obtained after $k=9$ steps of the iteration procedure (leading after four steps to Fig. 2b). This object had 1,048,576 touching points and 10,000 of these were selected randomly as centers for the circles within which the mass (the number of touching points) was determined. The results are shown in Fig. 5, where $\log \chi_q(r)/(q-1)$ is shown against $\log r$. Multifractality is indicated by parts of the curves having different slopes. For a structure with other parameter values the shape of the D_q spectrum is qualitatively the same, but the actual D_q values can be different.

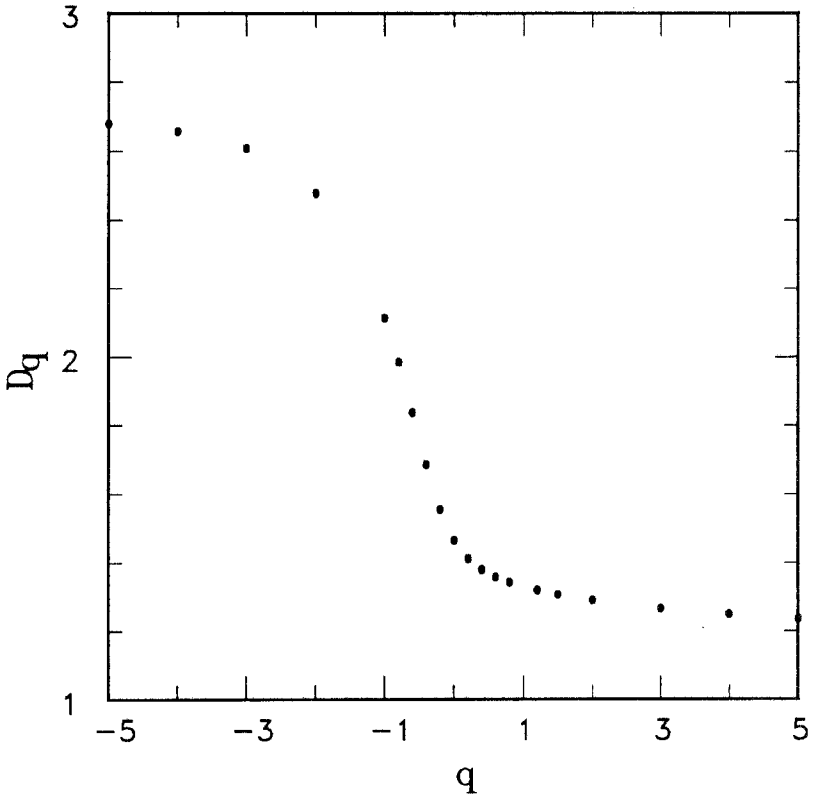

Fig. 6. The dependence of the generalized dimensions D_q on q as calculated from Fig. 5 for SFB.

The scaling is not satisfied for the full region of the r values, in accordance with the criterion that r has to satisfy $r_{\min} \ll r \ll r_{\max}$ in the scaling regime. There is a simple reason for the global behavior of the curves: all of them have to start and end up in the same point, since for $r_{\min}$ each circle contains only a single touching point, while for a radius equal to the system size each circle contains all of the points in the structure. Then, the curves may have straight parts with different slopes only if they depart from each other in a manner which is shown in Fig. 5.

The multifractal spectrum D_q is obtained by determining the slopes of the straight parts of the plots in Fig. 5. Our estimates are shown in Fig. 6. This figure has a remarkable feature: The D_q values for strongly negative values of q are larger than $d=2$, which is the embedding dimension. This question will be discussed later.

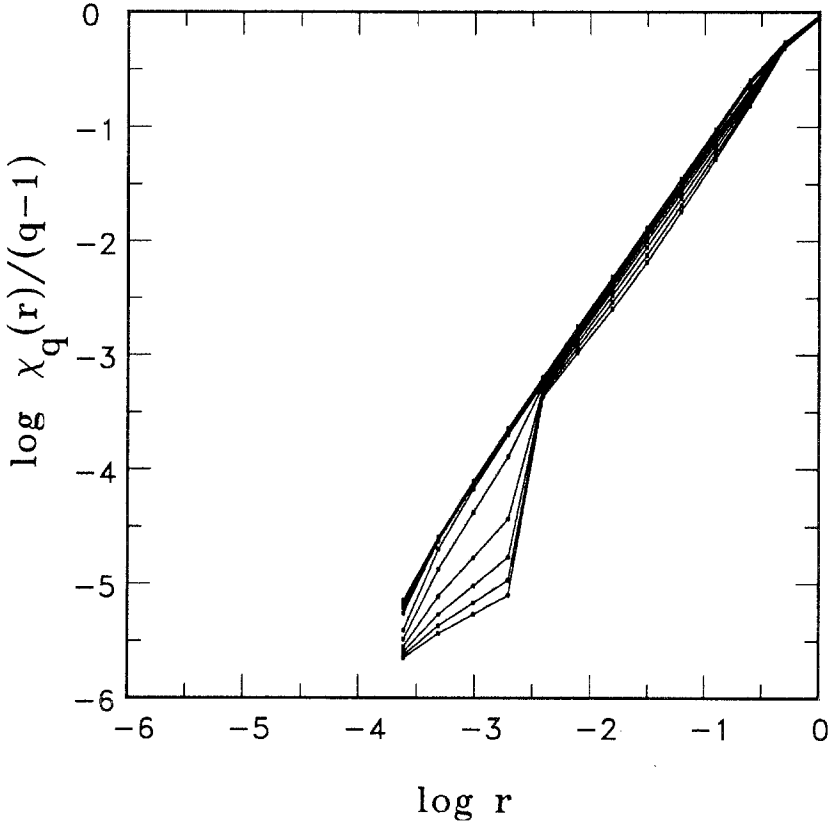

Fig. 7. The structure of SFB is monofractal if all of the circles down to a cutoff radius are included. In this case the slopes of the plots are approximately equal.

There is one more interesting feature of the multifractal analysis of SFB. This is related to the type of construction where all circles are included which have a radius larger than a lower cutoff radius $r_{\min}$. Obviously, in this case circles from a wide selection of generations occur in the final configuration even if the smallest circle is generated after only a few iterations. In such a structure the big empty regions tend to be filled up with circles coming from subsequent iterations (without including the circles with radii less then $r_{\min}$). As a result, the multifractal nature of the geometry is lost, as is demonstrated in Fig. 7, where the scaling of χ_q is shown for this case. The monofractality of the structure is indicated by the fact that the curves have the same slope.

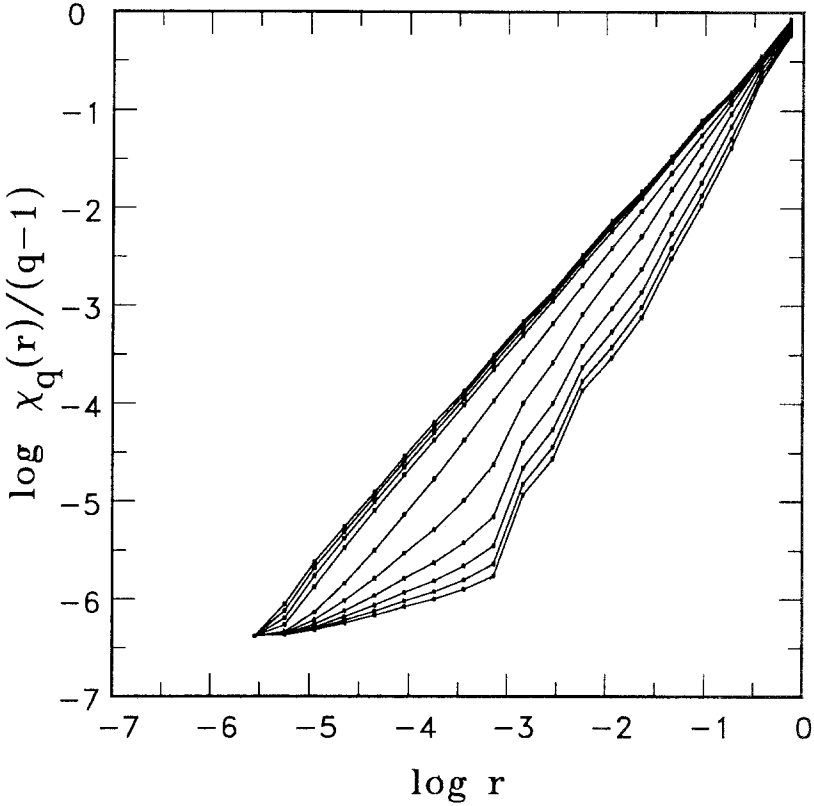

Fig. 8. The multifractal scaling of the distribution of the touching points demonstrated for the construction shown in Fig. 4. The generalized dimensions D_q can be determined from the slopes of the straight lines fitted to the data on the interval $-3.1 < \log r < -0.6$ for $q < 0$ and on the interval $-4.6 < \log r < -0.6$ for $q \geq 0$.

3.2. D_q Spectrum for the Apollonian Packing

In this section we present the results obtained for the scaling of the density of touching points in an Apollonian packing. The analysis is virtually the same as in the case of space-filling bearings. We start with three mutually touching circles of radii 1, 2, and 3. We went up to 12 generations, producing a total of 797,161 circles with 2,391,483 touching points and 10,000 centers were chosen randomly for the multifractal analysis. In addition, all of the remarks made for SFB concerning the special nature of the structures generated by a plane-filling fractal algorithm are valid for AP.

The multifractal nature of the Apollonian packing shown in Fig. 4 is demonstrated in Fig. 8, where $\log \chi_q(r)/(q-1)$ is plotted versus $\log r$ for various q.

The D_q spectrum calculated from Fig. 8 is shown in Fig. 9.

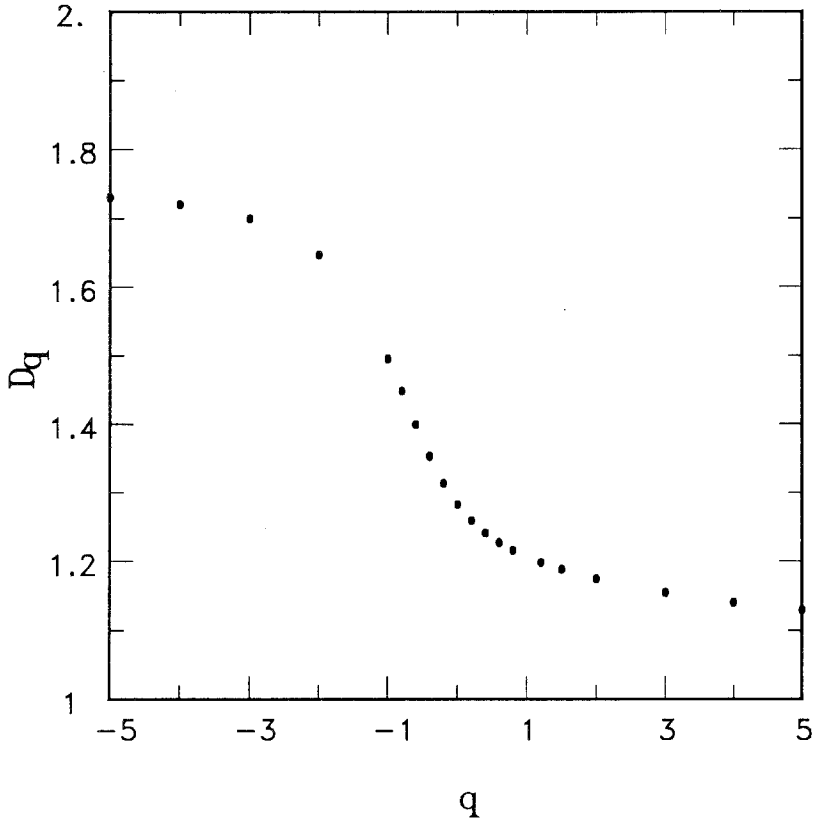

Fig. 9. The multifractal spectrum D_q for the touching points of Apollonian packing.

4. DISCUSSION

We have studied two types of plane-filling fractal structures made of circles; one of them (AP) is more than 2000 years old, the other one (SFB) has been proposed very recently. Our calculations show that the complex structure of these constructions is characterized by a spectrum of generalized dimensions.

The construction of the above fractals represents an iterative process in which different lengths are involved in a multiplicative manner. As a result, the distribution of the characteristic points (touching points) within the structures at a given stage of the process has multifractal properties, and a spectrum of q dependent generalized dimensions D_q can be associated with this distribution. The actual D_q values depend on the choice for the parameters of the models, but the qualitative behavior is the same in all cases. One of the surprising results is that D_q can be larger than d, where d is the embedding dimension. For a growing fractal it has been argued that $D_q \leqslant d$, since $D_{-\infty} = \alpha_{\max}$ and α can be considered as a local fractal dimension. The present model is, however, qualitatively different from particle growth models. It is generated by iterations, within a unit square.

More importantly, due to the nature of the construction, there exists *no such growth process* which would correspond to the blownup version of space-filling bearings. To illustrate this point, let us mention that in a growth model the already generated "inner" part is always frozen, and in the subsequent stages the new particles are added only to the outer parts. In the case of SFB and AP such a statement cannot be made; the newly generated parts always interpenetrate with the old parts. Correspondingly, the density of the touching points may exhibit arbitrary singularities in analogy with the distribution of return points in chaotic maps.[3]

We have also found that multifractality is absent in those versions of the models where all circles are included which have radii larger than some $r_{\min}(k)$ even if they appear at stages beyond the kth generation. The models of plane-filling disks have rich geometry and further investigations are expected to reveal additional interesting properties.

ACKNOWLEDGMENTS

We thank H. J. Herrmann for numerous helpful suggestions and T. Tél for useful discussions. T.V. is grateful for the hospitality extended to him during his stay at the supercomputing center in Jülich.

REFERENCES

1. B. B. Mandelbrot, *The Fractal Geometry of Nature* (Freeman, San Francisco, 1982).
2. T. Vicsek, *Fractal Growth Phenomena* (World Scientific, Singapore, 1989).
3. G. Mayer-Kress, ed., *Dimensions and Entropies in Chaotic Systems* (Springer, Berlin, 1986).
4. G. K. Bachelor, *Theory of Homogeneous Turbulence* (Cambridge University Press, 1982).
5. H. J. Herrmann, in *Correlations and Connectivity: Geometrical Aspects of Physics Chemistry and Biology*, H. E. Stanley and N. Ostrowski, eds. (Kluwer, Dordrecht, 1990), p. 108; H. J. Herrmann, G. Mantca, and D. Bessis, *Phys. Rev. Lett.* **65**:3223 (1990).
6. J. P. Hulin, A. M. Cazabat, E. Guyon, and F. Carmona, eds., *Hydrodynamics of Dispersed Media* (North-Holland, Amsterdam, 1990).
7. C. Sammis, G. King, and R. Riegel, *Pure Appl. Geophys.* **117**:1441 (1982).
8. B. B. Mandelbrot, *J. Fluid. Mech.* **62**:331 (1974).
9. U. Frisch and G. Parisi, in *Turbulence and Predictability in Geophysical Fluid Dynamics and Climate Dynamics*, M. Ghil, R. Benzi, and G. Parisi, eds. (North-Holland, Amsterdam, 1985).
10. T. C. Halsey, M. H. Jensen, L. P. Kadanoff, I. Procaccia, and B. Shraiman, *Phys. Rev. A* **33**:1141 (1986).
11. D. W. Boyd, *Mathematika* **20**:170 (1973).
12. S. Mertens, *J. Stat. Phys.* **58**:1095 (1990).
13. G. Huber, in *Correlations and Connectivity: Geometrical Aspects of Physics Chemistry and Biology*, H. E. Stanley and N. Ostrowski, eds. (Kluver, Dordrecht, 1990), p. 322.
14. T. Tél, *Z. Naturforsch.* **43a**:1154 (1988).
15. T. Tél and T. Vicsek, *J. Phys. A* **20**:L835 (1987).
16. T. Tél, A. Fülöp, and T. Vicsek, *Physica A* **159**:155 (1989).
17. T. Vicsek, F. Family, and P. Meakin, Multifractal geometry of diffusion-limited aggregates, *Europhys. Lett.* **12**:217 (1990).
18. S. S. Manna and H. J. Herrmann, *J. Phys. A* **24**:L481 (1991).